# Non-invasive measurements for characterization of *Hermetia Illucens* (BSF) life cycle in rearing plant


Massimiliano Proietti
Idea-Re S.r.l.
Perugia, Italy
mproietti@idea-re.eu

Andrea Marini
Idea-Re S.r.l.
Perugia, Italy
amarini@idea-re.eu

Alberto Garinei
Department of Engineering Sciences,
Guglielmo Marconi University,
Rome Italy
Idea-Re S.r.l.
Perugia, Italy
a.garinei@unimarconi.it

Gianluca Rossi
Department of Engineering
Università degli Studi di Perugia
Perugia, Italy
gianluca.rossi@unipg.it

Federico Bianchi
Idea-Re S.r.l.
Perugia, Italy
fbianchi@idea-re.eu

Marcello Marconi
Department of Engineering Sciences,
Guglielmo Marconi University,
Rome Italy
Idea-Re S.r.l.
Perugia, Italy
Perugia, Italy m.marconi@unimarconi.it

Silvia Discepolo
Dipartimento di Ingegneria Industriale e
Scienze Matematica (DIISM), Università
Politecnica delle Marche
Ancona, Italy
s.discepolo@pm.univpm.it

Maria Teresa Calcagni
Dipartimento di Ingegneria Industriale e
Scienze Matematica (DIISM),
Università Politecnica delle Marche
Ancona, Italy
m.t.calcagni@staff.univpm.it

Paolo Castellini
Dipartimento di Ingegneria Industriale e
Scienze Matematica (DIISM), Università
Politecnica delle Marche
Ancona, Italy
p.castellini@staff.univpm.it

Milena Martarelli
Dipartimento di Ingegneria Industriale e
Scienze Matematica (DIISM), Università
Politecnica delle Marche
Ancona, Italy
m.martarelli@staff.univpm.it

Giacomo Zeni
BugsLife S.r.l.
Perugia, Italy
zeni.giacomo@gmail.com

Stefano Speziali
Idea-Re S.r.l.
Perugia, Italy
sspeziali@idea-re.eu



2022 IEEE International Workshop on Metrology for Agriculture and Forestry (MetroAgriFor) | 978-1-6654-6998-2/22/$31.00 ©2022 IEEE | DOI: 10.1109/METROAGRIFOR55389.2022.9964687



***Abstract*— Black Soldier flies (BSFs) are very effective for the treatment of organic waste and their transformation into insect proteins and oils that can be used to produce feed and biofuels. An increasing number of startups and companies are breeding BSFs to take advantage of the numerous potential applications due to the larval diets. Although the breeding of BSF larvae requires artificially controlled conditions, methods for the characterization of the life cycle in production plan are lacking. Most of the analyses and procedures available in the literature cannot be used within the production lines of breeders. In the present study, an exploration of non-contact measurements (RGB video, thermal, Hyperspectral imaging) and of the analysis methodologies was carried out in order to identify the ones which are most significant for the different phases of the BSF life cycle, and which can be automated within the production lines. The result of the study was the definition of the criteria for the characterization, through non-contact measurements of the life cycle of the BSFs: computer vision algorithms based on image and data acquisitions were developed using 1) RGB camera for size / weight estimation and movement / vitality for the phases where the nutritional substrate is not present (pupae); 2) IR camera for the evaluation of movement / vitality for the phases where the nutrient substrate (larvae) is present and for the identification of temperature anomalies (metabolism too slow or too fast); 3) hyperspectral chamber to evaluate the growth of the larvae in relation to the chosen diet.**



***Keywords*— *Black Soldier flies, larvae, hyperspectral, thermal imaging, insect farming***


## I. INTRODUCTION

Black Soldier Flies (BSFs) are very effective for the treatment of organic waste. Their transformation into insect proteins and oils that can be used for the production of animal feed, biofuels and organic fertilizer. An increasing number of startups and companies are breeding BSFs to take advantage of the numerous potential applications due to the larval diets. A BSF female can lay between 200 and 700 eggs a time [1], which hatch in about 4 days [2]. Newborn larvae grow from 1 millimeter length and 0.10 g weight to 25 millimeters and 0.22 g during their larval stage that lasts from 18 to 36 days, depending on the food substrates provided and on the environmental conditions. BSF larvae are polyphagous, *i.e.*, they can be feed with a wide range of vegetal and animal substrates. The length of larval stage can be delayed by months due to low temperature or lack of food. Then larvae go through six instars before pupating. Pupal stage lasts from one to two weeks during which pupae stop eating and their mouths turn into suckers for water and nectar (sugar) [3]. Adults can survive for about ten days on fat reserves from larval stage.

According to Lalander *et al.* [4] the principal substrate properties affecting BSF larvae growing are proteins and volatile solids. Larvae grow slower with a low biomass conversion ratio on fruit & vegetable waste than with other substrates like animal feed and sludges. The amino acids profile of the prepupae did not vary greatly with the substrates. Studies in forensic entomology investigated the estimated colonization time to infer the elapsed time since death. In this context, Harden and Tomberlin [5] found that BSF larvae can


978-1-6654-6998-2/22/$31.00 ©2022 IEEE

be reared between 25 °C and 32 °C; temperatures above 36 °C can seriously harm larvae because they also generate themselves heat through their fast metabolism. Minimum accumulated degree hours (ADH) required by BSFs to complete the stages of their development (oviposition to hatch, hatch to prepupa, prepupa to pupa, pupa to adult) depend on diet provided and on the temperature of rearing. In [6] Chia and al. found that the thermal maximum for larval, pre-pupal and pupal development range between 37.2 ± 0.3 and 44.0 ± 2.3 ˚C (for BSF reared on spent grain with brewers' yeast substrate) while lower growing temperature threshold for larvae were 11.7 ± 0.9 and 12.3 ± 1.4 ˚C. In [7] Putra and Safa'at found that substrates used (different mix of fish offal, banana skin, tofu dreg) do not affect sex ratio of adult flies and weight of pupae is a better predictor of sex than length. BSF females tend to be produced from pupae with a higher length and weight.

BSF rearing is a rapid growing business but to be economically feasible some factors need to be considered: waste to larvae biomass rate conversion, mating and oviposition. These factors essentially depend on the quality and availability of nutrients, on the environmental conditions. These aspects need to be carefully and continuously monitored in a production plant.

In order to gather information about the BSF life cycle during the rearing in a production plant a methodology that makes use of measurements without making physical contact with BSFs is needed. NIR (Near Infrared) technologies are successfully used to estimate protein contents in food [8] and in insects [9]. In [8] Béc et al. uses three consumer-grade NIR spectrometers (with spectrum between 12500-4000 $cm^{-1}$, 11013-5967 $cm^{-1}$, 13514-9346 $cm^{-1}$) to successfully analyze insect protein content of handcrafted fitness bars through non-invasive measurements. In [9] Hou et al. used Fourier-transform infrared spectroscopy and machine leaning to effectively predict amino acids content of nine commercial insects: Tenebrio molitor, Zophobas morio, Locusta migratoria, Bombyx mori, Teleogryllus emma, Acrida cinerea, Chrysomya magacephala, Hemetia illucens (BSF) and Musca domestica. Hyperspectral remote sensing was used in [10] to examine the effects of different food substrates on the development times of Lucilia sericata through the effects on the hyperspectral measurements of post feeding. In [11] Johnson and Wallman used thermal imaging to locate maggot mass within a carcass and estimate associated maggot mass temperature providing useful information for predicting larvae grow rates.

Machine Learning and Deep Learning for computer vision provide efficient solutions to perform continuous and non-invasive entomological observations throughout diurnal and seasonal cycles [12]. Hansen at al. [13] trained an SSD-MobilenetV2 neural network for object detection to count and measure size of BSF larvae. The dataset was formed by NIR images and RGB images. Acquisition and object detection systems were developed on a Raspberry Pi which can work in edge mode. The mean Average Precision of the model was around 87%.

In this study we identify a preliminary set of non-contact measurements needed to characterize the BSF gender in a herd. Measurements and subsequent data processing are designed to be automated and to be performed in the production line, *i.e.* by means of edge computing devices.

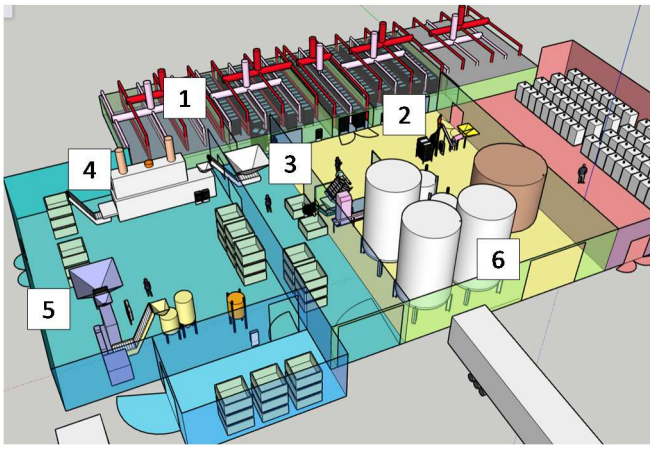


*Figure 1: rearing plant schema*

Rearing plant, as in Figure 1, where the study is conducted has the following areas: 1) feeding floor where larvae grow; 2) harvesting of larvae and substrates; 3) separation of mature larvae from substrates; 4) drying kiln; 5) rendering zone where fats are separated and the resulted larvae's proteins are milled and packaged; 6) silos for larvae feed.

The process if rearing in the plant is described in the following. Same day eggs from different fly cages are harvested. Newborns from eggs are collected in boxes with food substrate and form starter larvae. After 5-7 days developed larvae are separated in two parts: one for drying and one for reproduction. Larvae for reproduction are placed in a pre-pupal room where they are feed again. After the pre-pupal stage, they are placed in a pupal room where they are subjected to intervals of light and dark. Pupae at the end of pupal stage are placed in cages where fly adults emerge.

## II. MEASUREMENT SET-UP

### *A. Hyperspectral image measurement set-up*

An HinaLea hyperspectral camera, model 4250 VNIR, has been used in conjunction with an illumination system consisting of two halogen lamps arranged in a configuration with an angle of incidence of 45° (Figure 2). Despite the good light coverage provided by the halogen source, its sensitivity decreases in wavelengths above 880 nm (Figure 3). The camera works in the VIS-NIR (Visible and Near Infra-Red) wavelength range from 412 to 998 nm with a spectral resolution of 2 nm. The camera hosts a CMOS sensor has a resolution of 668 x 998 pixels to operate at a minimum operating distance of 20 cm).

The hyperspectral camera allows to acquire hypercubes collecting the images representing the reflectance of the framed object at the different wavelengths of the spectrum.

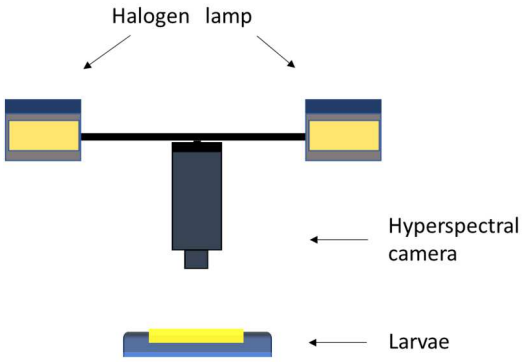


*Figure 2: The measurement set-up for the hyperspectral image acquisition including the illumination system*

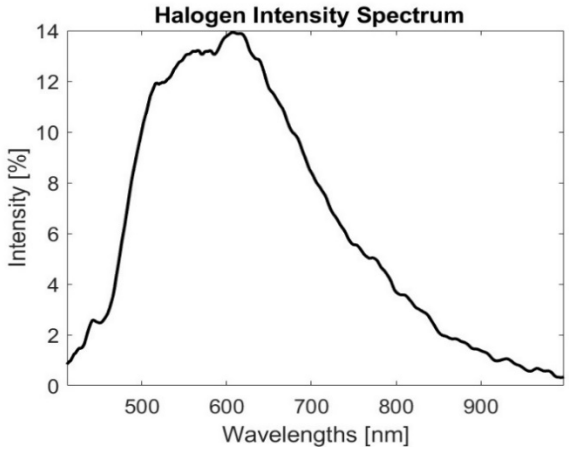


*Figure 3: Halogen Intensity spectrum*

### *B. RGB and LOW-RES IR image set-up*

A remote sensing station equipped with RGB camera (picamera 1.3, 3280x2464 pixels, full HD videos), and a low-resolution thermal camera (FLIR Lepton 160x120 pixels) is placed about 40 cm away from the feeding vessel. The sensing station has an edge device (Raspberry PI 4) for the computations needed on the cameras data (Figure 4).

### *C. HIGH-RES IR image set-up*

As shown in Figure 4 high resolution FLIR A6751sc thermal camera (640x512 pixels) is placed similarly to the hyperspectral and RGB/IR devices, in order to take images normally with respect to the larvae-substrate surface.

## III. DATA COLLECTION

### *A. Hyperspectral data collection and methods*

The enumerated pupae are placed twenty at a time on a white sheet of size 10 cm x 7 cm (Figure 5). These dimensions are selected both to match the working distance of the camera of about 32 cm and to fill the entire field of view of the device. Prior to each acquisition, the flat and black calibration procedure is performed for reflectance measurements. The first calibration is made via a specific optical target placed in

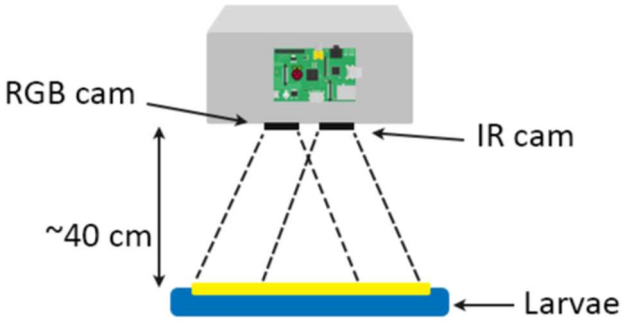


*Figure 4: Measurement set-up for RGB and LOW-RES IR cameras*

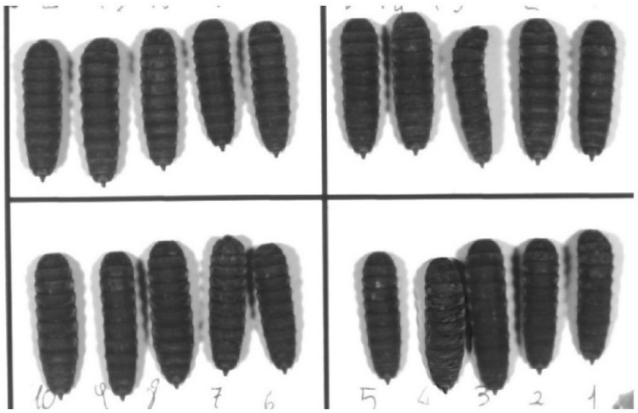

*Figure 5: Pupae acquisition set-up*

front of the sensor, and the second by closing the camera lens. For each hyperspectral image acquired, the area belonging to the pupa is selected automatically by the following procedure. The acquired image is divided into four quadrants with five pupae each. For every section, exploiting the different pupae intensity value (value: 0, color map in Figure 6) with respect to the background (value: 1, color map in Figure 6), the sum of all pixels along the vertical direction of the image is performed to find the object of interest in this study. To highlight the region of pupae, the peak corresponding to each pupa is computed by subtracting the sum intensity value from the maximum of the sum intensity value:

$$max(s(I(Y)) - s(I(Y)). \quad (1)$$

The ROI is defined for all pupae with a constant rectangular shape (Figure 6). Starting from the intersection of the mean pixel value along the y-axis and the previously identified peaks, a centroid point inside each pupa is found. Moving from that, 6 pixels on the left and right side from the centroid are chosen to trace the base of the rectangle, and 30 pixels on the top and bottom to identify the height of the ROI. As a result, the ROI of each pupa is featured by a value of 793 pixels.

Once the ROIs are mapped out, the average spectra of each region are extracted from the hyperspectral cube. Known the gender data of each pupa, from the sex monitoring campaign, the male and female spectra pupae are compared. In data collection, some pupae are omitted for the following reasons: pupae whose sex is uncertain, pupae that died, and lastly

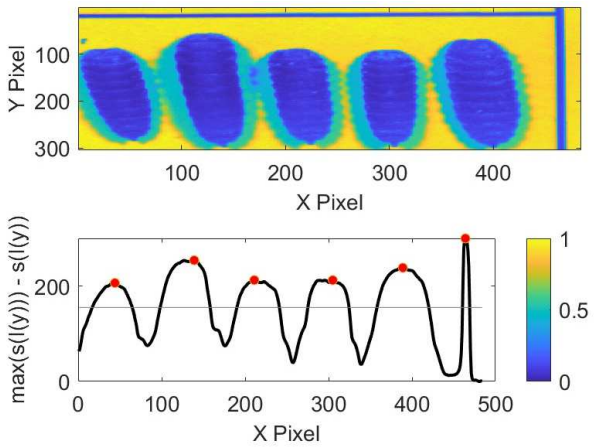


*Figure 6: Peaks identification*

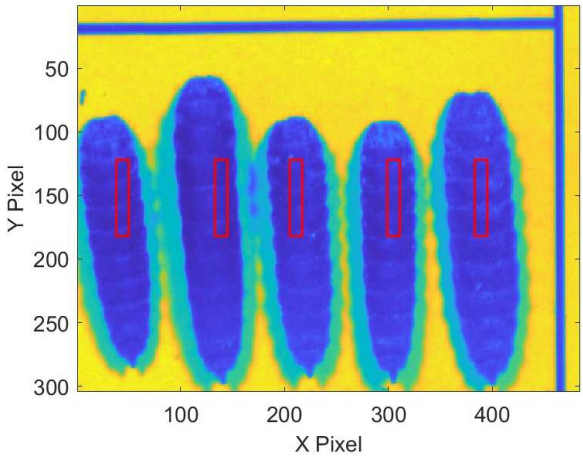


*Figure 7: Pupae ROI extraction*

those pupae that due to incorrect positioning in the white sheet had a ROI that is not centered in the pupa itself. From the mean value of male and female spectra, the respective standard deviations are calculated.

### *B. Thermal images acquisition and features extraction*

The experiments were conducted in a room that had a controlled ambient temperature (24 ± 3 °C) and variable but typically low relative humidity, between 20% and 40%.
20 adult BSFs at a time (Figure 8) were kept inside a 10cm x 7cm box acquiring images of both the front (f) and the back (r). The thermal camera was placed at 40 cm from larvae, distance that was determined to ensure that the pupae were of suitable size in the images. Images were captured with the maximum resolution possible.
In total, 120 front images and 120 back images of single larvae were acquired and used for classification analysis.
The IR camera provides a value of temperature for each pixel, but, since the emissivity of each pupa is not known, the monitored temperature cannot be used as an absolute value.
The pupae images were manually cropped to obtain individual images (Figure 9a). To highlight only the pixels belonging to the pupae and thus show the peculiarities of the image, without considering the background, adaptive masks were created by applying a threshold to the distribution of the

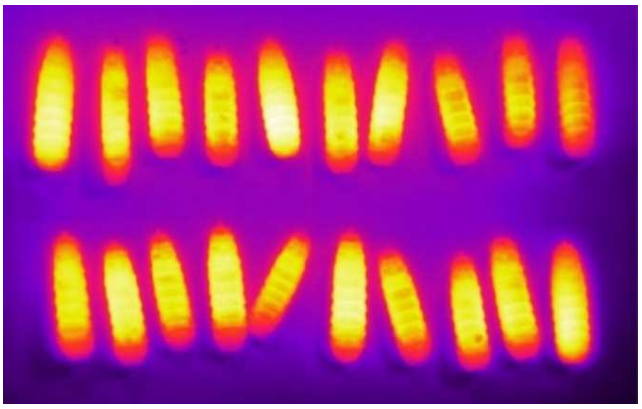

*Figure 8: Thermal images acquisition set-up*

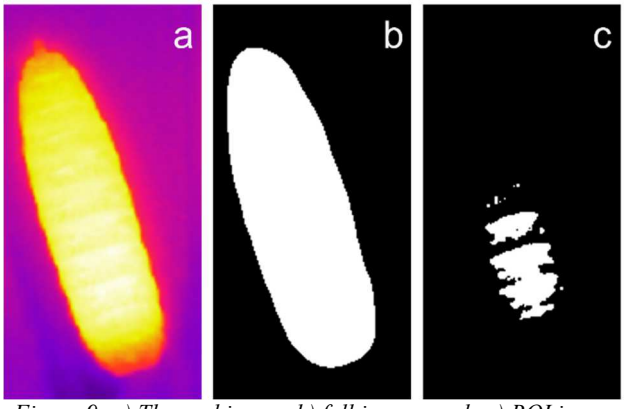


*Figure 9: a) Thermal image. b) full image mask. c) ROI image mask.*

intensity of the grayscale image (Figure 9b).
In addition to the total image, a ROI (Figure 9c) relative to the hottest area was taken into consideration for each pupa, making a cut at the 85th percentile in the intensity scale.
About 1500 radiomic features related to both the total image and the ROI were extracted for each image. Radiomics focuses on image analysis enhancements, using automated throughput extraction of large amounts of image features. A quantitative analysis of the image data can provide a great deal of additional information. For the original image, its derivative and the filtered wavelet, the extracted feature classes are: first order, glcm, glrlm, glszm, gldm, ngtdm. Such features describe morphological and predictive characteristics that can be divided into two groups: dimensions and properties based on morphology (first order) and descriptors of the relationships between the pixels that make up the image (glcm, glrlm, glszm, gldm, ngtdm).
The whole procedure was applied to the front and back images. The feature sets were indexed with 'f' and 'b' and concatenated, being corresponding to the same sample. Weight and length have also been added to the aforementioned features.
Labeling of pupae in females (F) and males (M) was performed after image acquisition at the death of the flies. Pupae with uncertain sex and those that died were not considered in the dataset.
The set of features has been reduced up to 400 by an unsupervised analysis, eliminating the features with correlation coefficient > 0.9, and the constant and quasi-

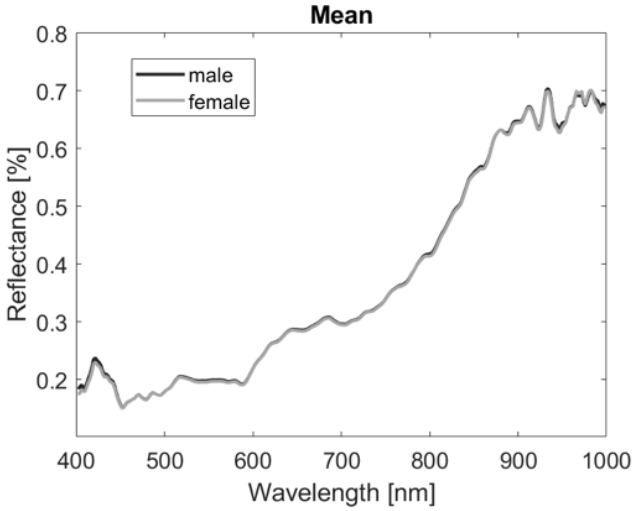


*Figure 10: Mean gender spectra*

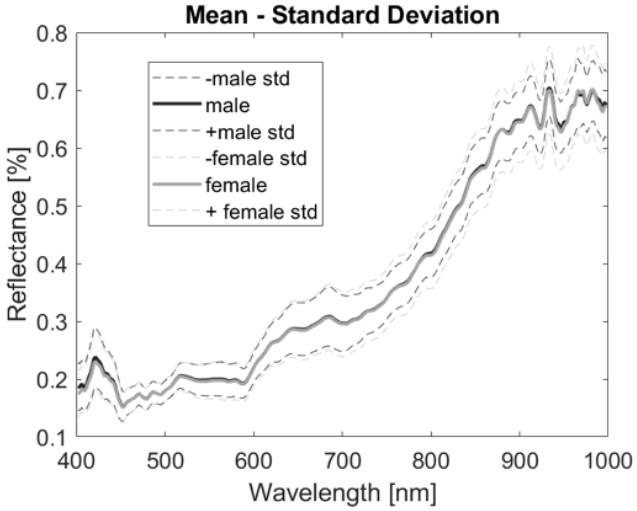


*Figure 11: Mean and standard deviation of gender spectra*

constant features, thus maintaining only features with a variance ≠ 0.

In addition, for each feature, using the labeled output, the Kruskal-Wallis test was performed. Statistical significance was set at p-value < 0.05. A set of 22 features with p-value < 0.05 was selected for subsequent analysis.

Three machine learning methods: Logistic Regression, Random Forest and a Support Vector Machine (SVM) were implemented to build prediction models.

The dataset was not subject to balance resampling since the balancing ratio is equal to 0.95.

A Train:Test split of 85:15 was used. To increase the robustness of prediction models, for each of the three models, a 10-fold cross validation was implemented, and the optimal parameters were chosen based on F1-score (harmonic mean of the precision and recall).

To further reduce the dimensionality of the dataset, a principal component analysis (PCA) was carried out, the selected number of components was set equal to 0.95, such that the amount of variance that needs to be explained is greater than that value. The dataset was reduced to 5 features.

We present our validation results in terms of accuracy (Equation 1), true positive rate (Equation 2) and true negative rate (Equation 3):

$$Accuracy = \frac{TP+TN}{TP+TN+FP+FN} \quad (1)$$

$$True\ Positive\ Rate = \frac{TP}{TP+FN} \quad (2)$$

$$True\ Negative\ Rate = \frac{TN}{TN+FP} \quad (3)$$

where TP are the true positives, TN are the true negatives, FP are the false positives and FN the false negatives.

## IV. RESULTS

### A. Hyperspectral Results

Figure 10 shows the male and female mean spectra: the two genders are separated, but Figure 11 reveals that due to the high standard deviation value the two genders do not appropriately differentiate.

It appears that, as of now, the hyperspectral system cannot appropriately discriminate between the two genders. This study can be improved going to analyze the entire pupa region and not just a ROI of interest, and by improving the illumiation system.

### B. Thermal Imaging Results

The model performances using different machine learning methods based on two different input variables are shown in Tables 1.

*Table 1. Model performances*

| Classifier | Accuracy | TPR | TNR |
|---|---|---|---|
| Logistic Regression | 0.68 | 0.72 | 0.63 |
| Random Forest | 0.65 | 0.62 | 0.67 |
| SVM | 0.61 | 0.93 | 0.26 |

The best performing model appears to be the logistic regression which has the highest accuracy value. It should be noted that the Random Forest and SVM classifiers, among the tested models, show high values of TPR and TNR despite having lower accuracy values. These results, although preliminary, show on the one hand the feasibility of the procedure followed in the recognition of the female and male pupae of BSFs and on the other hand they suggest continuing the study by increasing the number of samples available, also exploring different models in the description of the datasets. This analysis would be important for any commercial implementation.

## V. CONCLUSIONS

In this study we have developed a method for the genus characterization of BSF employing non-contact measurements that can be used in the production lines of a breeding facility in an automated manner. This is a first step to improve efficiency in production lines based on food and environmental conditions.

## REFERENCES


[1] Tomberlin, J. K., Sheppard, D. C. & Joyce, J. A. "Selected life-history traits of black soldier ies (diptera: Stratiomyidae) reared on three arti cial diets." Annals of the Entomological Society of America 95, 379{386 (2002).

[2] Sheppard, D. C., Tomberlin, J. K., Joyce, J. A., Kiser, B. C. & Sumner, S. M. "Rearing methods for the black soldier y (diptera: Stratiomyidae)." Journal of Medical Entomology 39, 695{698 (2002).

[3] Myers, H. M., Tomberlin, J. K., Lambert, B. D. & Kattes, D. "Development of black soldier y (diptera: Stratiomyidae) larvae fed dairy manure." Environmental entomology 37, 11{15 (2014)

[4] Lalander, C., Diener, S., Zurbrügg, C., & Vinnerås, B. (2019). "Effects of feedstock on larval development and process efficiency in waste treatment with black soldier fly (Hermetia illucens)." Journal of cleaner production, 208, 211-219.

[5] Harnden, L. M. & Tomberlin, J. K. "Effects of temperature and diet on black soldier y, hermetia illucens (l.)(diptera: Stratiomyidae), development." Forensic science international 266, 109{116 (2016).

[6] Chia, S. Y., Tanga, C. M., Khamis, F. M., Mohamed, S. A., Salifu, D., Sevgan, S., ... & Ekesi, S. (2018). "Threshold temperatures and thermal requirements of black soldier fly Hermetia illucens: Implications for mass production." Plos one, 13(11), e0206097.

[7] Putra, R. E., & Safa'at, N. (2020). "Study on Sex Determination and Impact of Sex Ratio to Reproduction Success in Black Soldier Fly." Jurnal Biodjati, 5(2), 191-198.

[8] Beć, K. B., Grabska, J., Plewka, N., & Huck, C. W. (2021). "Insect protein content analysis in handcrafted fitness bars by NIR Spectroscopy. Gaussian process regression and data fusion for performance enhancement of miniaturized cost-effective consumer-grade sensors." Molecules, 26(21), 6390.

[9] Hou, Y., Zhao, P., Zhang, F., Yang, S., Rady, A., Wijewardane, N. K., ... & Li, M. (2022). "Fourier-transform infrared spectroscopy and machine learning to predict amino acid content of nine commercial insects." Food Science and Technology, 42.

[10] Warren, J. A., Ratnasekera, T. P., Campbell, D. A., & Anderson, G. S. (2018). "Hyperspectral measurements of immature Lucilia sericata (Meigen)(Diptera: Calliphoridae) raised on different food substrates" Plos one, 13(2), e0192786.

[11] Johnson, A. P., & Wallman, J. F. (2014). "Infrared imaging as a non-invasive tool for documenting maggot mass temperatures." Australian Journal of Forensic Sciences, 46(1), 73-79.

[12] Høye, T. T., Ärje, J., Bjerge, K., Hansen, O. L., Iosifidis, A., Leese, F., ... & Raitoharju, J. (2021). "Deep learning and computer vision will transform entomology." Proceedings of the National Academy of Sciences, 118(2).

[13] Hansen, M. F., Oparaeke, A., Gallagher, R., Karimi, A., Tariq, F., & Smith, M. L. (2022). "Towards Machine Vision for Insect Welfare Monitoring and Behavioural Insights." Frontiers in Veterinary Science, 9.